Development and Testing of Temperature-sensitive Beads for Simultaneous Thermometry and Velocimetry

Trenton J West

A thesis
submitted in partial fulfillment of the
requirements for the degree of

Master of Science
in
Aeronautics and Astronautics

University of Washington
2012

Committee:
Dana Dabiri, Chair
Gamal Khalil

Program Authorized to Offer Degree:
Aeronautics and Astronautics

The views expressed in this article are those of the author and do not reflect the official policy or position of the United States Air Force, Department of Defense, or the U.S. Government.

University of Washington

Abstract

Development and Testing of Temperature-sensitive Beads for
Simultaneous Thermometry and Velocimetry

Trenton J West

Chair of the Supervisory Committee:
Dana Dabiri
Department of Aeronautics and Astronautics

Temperature-sensitive beads (TSBs) have been developed with promising characteristics for application to complex flows, giving the capability for flow visualization via simultaneous full-field thermometry and velocimetry. The buoyant plume resulting from natural convection was selected as the flow for preliminary testing. Of the various TSBs fabricated and tested, the best results were achieved with 5 μm-diameter polystyrene microspheres doped with Europium (III) thenoyltrifluoroacetonate (EuTTA) and Coumarin. The dual-dye sensors rely on the temperature-sensitive luminescence of EuTTA for thermometry, while the temperature-insensitive Coumarin serves as a reference dye, allowing for correction of non-uniformities in lighting and particle size/shape. The TSBs are shown to meet particle size, particle response time, particle density, and temperature sensitivity requirements for natural convection in water. Moreover, the characteristics of the TSBs are suitable for a variety of turbulent water flows. A thermal response time has yet to be measured for the TSBs, but an appropriate technique for performing this measurement is in development.

TABLE OF CONTENTS

LIST OF FIGURES

LIST OF TABLES

ACKNOWLEDGEMENTS

I would like to extend a special thank you to Professor Dana Dabiri and Professor Gamal Khalil for their support of my research and for facilitating me in earning my Master of Science degree. This achievement would not have been possible without their guidance and assistance. In addition, I thank Professor Younan Xia and Cun Zhu of Washington University in St. Louis for their collaboration in the development of TSBs. I thank my classmate and friend, Micah Paul, for his assistance in performing PIV analysis. I also thank Kristina Wang, Guoshi Li, Alex Perez, Wei-Hsin Tien, and the other research assistants for their daily help and contribution to my research. I thank my father and mother for their encouragement and support throughout my life and during my time here in Seattle. Most importantly, I give all praise and glory to the Lord God Almighty; for saving me with the blood of Jesus Christ, for carrying me back to His fold when I wandered away, and for sustaining me, now and forevermore.

Chapter 1. INTRODUCTION

Fluid mechanics is the study of fluids and the forces exerted on them. Generally, the determination of these forces is performed indirectly, through analysis of physical fluid properties such as pressure, temperature, velocity, etc. Within thermofluidic flows, temperature is a variable of primary importance, as the name might suggest. Moreover, velocity is of great importance in these flows. Knowledge of these variables is vital to achieving any level of understanding of the primary mechanisms at work in a complex flow. Accordingly, accurate measurements of temperature and velocity are necessary.

In the acquisition of temperature and velocity data within a complex flow, one of the most essential features of a sensor is that it be non-intrusive. Preservation of flow features is critical to experimental fidelity and great care must be taken to ensure that the physical presence of a sensor does not significantly alter the flow. Therefore, the measurement technique/instrument must be carefully selected depending on the experimental conditions. A wide array of sensors for measuring temperature and velocity exist and a few such options are presented.

1.1 THERMOMETRY

Temperature measurement is an inherently difficult process. Errors in thermometry often occur due to temperature gradients, sensor self-heating, radiation, or a number of other complicating phenomena. Furthermore, for complex flows with high frequency temperature fluctuations due to turbulent transport, the thermal time constant for a sensor is often the limiting factor. Three of the most common types of temperature sensors are thermocouples, resistance temperature detectors, and infrared thermometers.

1.1.1 *Thermocouples*

A thermocouple consists of two dissimilar metals connected at an interface. This interface is known as a thermoelectric junction. A thermocouple operates on the principle that a temperature change at the thermoelectric junction generates an electromotive force proportional to the temperature difference. This phenomenon, known as the Seebeck effect, was discovered by Thomas Johann Seebeck in the early 1800s [1]. By completing the thermoelectric circuit with a voltage measurement device, changes in temperature can be measured as changes in voltage.

One particular type of thermocouple is the thin-film thermocouple. In this design a very thin film of metal is deposited onto a dissimilar metal, forming a thermoelectric junction at the tip of a probe. In order for temperature changes to be sensed, heat must penetrate through the thin film layer to the junction. As a result, the key factor in determining the thermal time constant of this thermocouple is the film thickness. According to McIntosh, film thicknesses on the order of μm are required for a thermal time constant on the order of microseconds [2]. While thin-film thermocouples can be designed to have microsecond time constants, their manufacture, specifically the deposition of the thin-film, proves challenging.

1.1.2 *Resistance Temperature Detectors*

A resistance temperature detector (RTD) generally consists of an electrically conductive material etched on a semi-conductive substrate. Additionally, RTD's often take the form of a heat transfer gauge, where a thin film of metal is deposited on a substrate. An RTD operates on the principle that a temperature change alters the electrical resistance of the conductor. A simple circuit involving the RTD, additional resistors, and a constant current or voltage supply can be built wherein changes in temperature cause changes in the resistance of the RTD, which in turn can be measured as changes in voltage. When compared to thermocouples, RTD's are usually larger, more expensive, and have a slower response time [3].

Thermistors also fall under the category of RTD's. A thermistor consists of a ceramic or polymer semi-conductor with resistance that is sensitive to temperature. Thermistors exhibit high sensitivity to temperature changes, but their resistance changes non-linearly and they are effective over a small temperature range. Furthermore, thermistors generally have a large thermal time constant.

1.1.3 *Infrared Thermometers*

An infrared thermometer is a device that measures the intensity of electromagnetic radiation emitted by a body. Infrared thermometry relies on the principle that any object emits electromagnetic radiation as a function of its temperature. A typical infrared thermometer will at least consist of an optical system to gather emissions and additional hardware for signal conversion and recording. One major benefit of infrared thermometry is its non-intrusive nature, which allows for temperature measurements to be made at very high temperatures. The main

drawback of infrared thermometry is high cost due to the high complexity of the measurement system.

1.1.4 *Full-field Thermometry*

While thermocouples and resistance temperature detectors are extremely useful temperature sensors with a wide variety of applications, one major shortcoming is their inability to perform full-field measurements. Both thermocouples and RTD's are point-wise sensors, meaning that one sensor provides temperature data at one point in space. Consequently, the temperature at all other points in the flow are unknown. While this deficiency can be overcome by employing arrays of thermocouples or RTD's throughout the flow, this practice is generally less than ideal due to the ensuing high cost and complexity. Infrared thermometers can, in fact, provide full-field measurements in a non-intrusive manner. However, the infrared thermometry systems are extremely complex and expensive, and they generally lack adequate temporal resolution. Therefore, traditional temperature measurement instruments/techniques do not meet the need for full-field, non-intrusive, high temporal resolution data acquisition, so alternative methods must be explored.

1.1.5 *Temperature-sensitive Paint*

The concept of luminescent thermometry using temperature-sensitive paint has its origin in luminescent barometry. Luminescent barometry was developed and patented at the University of Washington in collaboration with NASA-Ames Research Center beginning in the 1980's [4]. Initially, surface-based luminescent paint was used to make pressure measurements relying on the concept of oxygen quenching. The intensity of the luminescence of dye molecules decreases as pressure, and thus oxygen quenching, increases, and the relationship between intensity and local air pressure can be expressed by the Stern-Volmer equation as

$$\frac{I_o}{I} = A + B\left(\frac{P}{P_o}\right), \tag{1.1}$$

where I_o is intensity at known pressure P_o, and I is intensity at pressure P [4]. Using this relationship, luminescent barometry was implemented to map surface pressure fields using video imaging detection.

With the powerful full-field capability of luminescent barometry in hand, the exploration of luminescent thermometry was a fairly intuitive second step. Distinct applications for

luminescent thermometry existed in the field of aerodynamics, especially in measuring heating and boundary layer transition. Accordingly, efforts were undertaken for the development of surface-based luminescent paint for thermometry.

Temperature-sensitive paint is an experimental thermometry technique consisting of luminescent molecules that operate based on the mechanism of thermal quenching. Figure 1.1 shows a schematic of a typical surface-based luminescent paint. A luminescent molecule is excited when it absorbs high-energy light, usually within the ultraviolet spectrum. The molecule generally returns to its ground state by emitting light. Additionally, a luminescent molecule is capable of returning to its ground state by a radiationless decay mechanism. As temperature increases, the likelihood of an excited molecule returning to ground state via radiationless decay increases, which is the concept of thermal quenching. Accordingly, the intensity of emitted radiation decreases as temperature increases. For a specific temperature range, the Arrhenius form can be used to define the relation between luminescent intensity I and absolute temperature T as

$$ln\frac{I(T)}{I(T_{ref})} = \frac{E_{nr}}{R}\left(\frac{1}{T} - \frac{1}{T_{ref}}\right) \tag{1.2}$$

where E_{nr} is the activation energy for the radiationless process, R is the universal gas constant, and T_{ref} is a reference temperature in Kelvin [5].

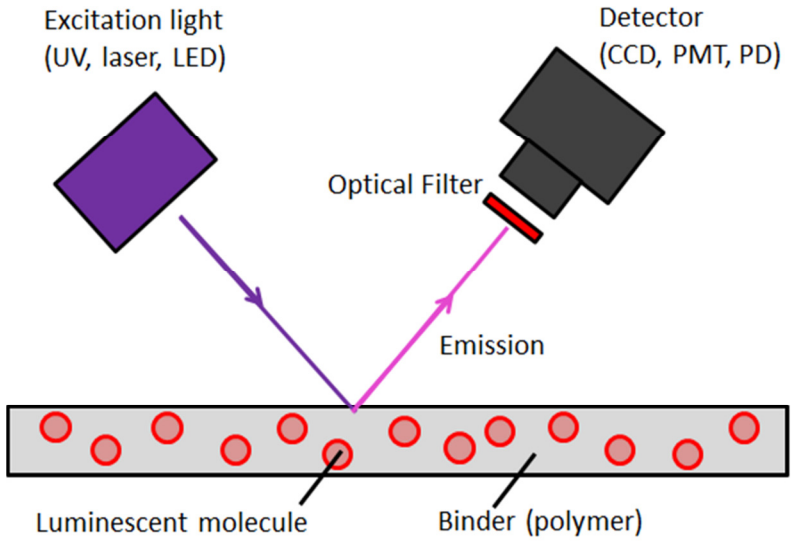

Figure 1.1 Schematic of luminescent surface paint (adapted from [5])

The major merits of temperature-sensitive paint are its ability to provide non-intrusive, full-field thermometry. The sensor is non-intrusive because it can be smoothly applied to a surface of interest with minimal alteration of the flow over the surface. Furthermore, the paint provides full-field thermometry because the temperature can be determined for every point where the paint is applied based on the luminescence of molecules at each point. As a result of its non-intrusive, full-field qualities, temperature-sensitive paint warrants serious investigation for use as a temperature sensor in complex flows.

1.2 VELOCIMETRY

Velocimetry, like thermometry, is not a trivial endeavor. Determining the velocity of a fluid without considerably altering the flow is quite challenging. Differential pressure sensors and velocity anemometers are common sensors for velocity acquisition.

1.2.1 *Differential Pressure Sensors*

Differential pressure sensors most commonly take the form of pitot tubes. A pitot tube is a fairly simple device generally consisting of a tube with one opening normal to the fluid flow and one opening parallel to the flow. At the opening normal to the flow, the fluid is brought to stagnation and the result is a measurement of total pressure. At the opening parallel to the flow, the static pressure is measured. After determining the density of the fluid, Bernoulli's equation can be used to calculate the dynamic pressure, and subsequently the velocity. Pitot tubes are widely used in aerodynamics for their simplicity (no moving parts) and the capability to sample at high frequency.

1.2.2 *Velocity Anemometers*

The hot-wire anemometer is the most extensively used velocity anemometer in the world of aerodynamics. The sensor consists of a fine-gauge metal wire stretched normal to the flow. The wire is electrically heated to a temperature above the ambient temperature. When the fluid flows past the wire, cooling of the wire occurs in proportion to the velocity of the fluid. By monitoring the current, voltage, or temperature of the wire, the velocity of the fluid can ultimately be calculated. Although extremely delicate due to the fineness of the wire, hot-wire anemometers are valued for their capability for high frequency response.

1.2.3 *Full-field Velocimetry*

While differential pressure sensors and hot-wire anemometers are exceedingly useful velocity sensors with abundant employment in experimental aerodynamics, their primary shortcoming, as with conventional temperature sensors, is their inability to perform full-field measurements. Pitot tubes and hot-wires are point-wise sensors, measuring the velocity at a single point in the flow. The use of multiple sensors to perform velocimetry at multiple points is largely impractical without significantly modifying the flow. As such, alternate non-intrusive velocimetry methods must be sought.

1.2.4 *Particle Image Velocimetry*

Particle image velocimetry (PIV) is an experimental method based on the direct determination of the two fundamental dimensions of length and time [6]. Most commonly, tracer particles with a density similar to the fluid and of sufficiently small size are added to a fluid flow. The similar density allows for neutral buoyancy and the size ensures that the tracer particles closely follow the fluid motion. A quick sequence of light pulses can be used to illuminate the particles so that a high-speed camera can take images of the motion of the fluid. The velocity of individual particles is determined from the displacement of particles between consecutive images, leading to velocimetry throughout the flow. Figure 1.2 shows a schematic for a typical PIV experimental setup.

PIV is a powerful velocimetry technique for its non-intrusive and full-field qualities. PIV is an optical technique that does not interfere with the flow, and the tracer particles, if chosen appropriately, do not alter the flow. In addition, PIV provides velocity data throughout the entire flow. PIV has been utilized to visualize natural convection and vortex flows [7]. Common turbulent flows, such as the wake of a heated cylinder, have been extensively investigated using PIV techniques [8] [9] [10]. Consequently, PIV is a suitable method for velocity sensing in complex flows.

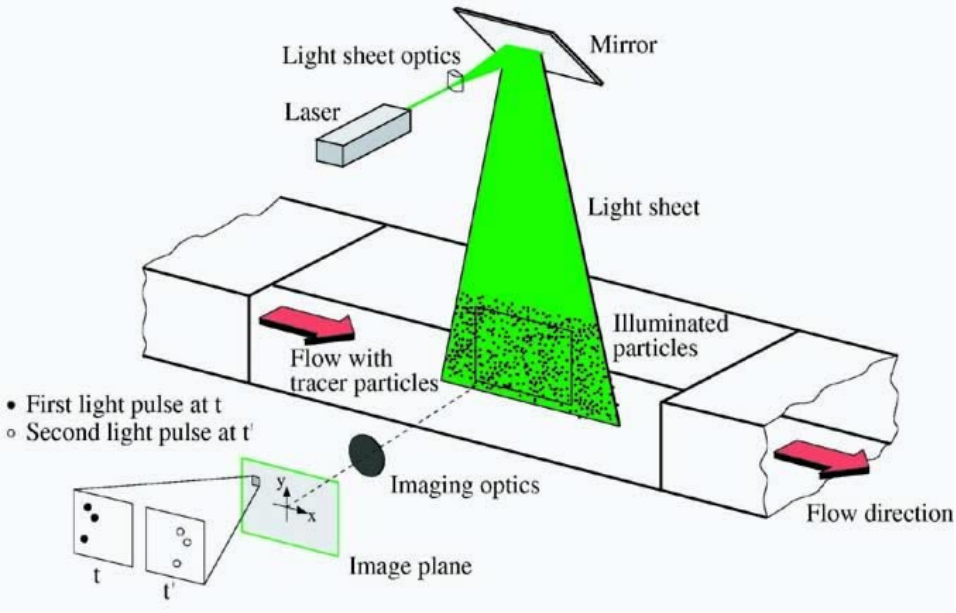

Figure 1.2 Experimental setup for particle image velocimetry [6]

1.3 MOTIVATION

An ideal experimental technique for visualization of turbulent thermofluidic flows is one in which velocimetry and thermometry are performed simultaneously, non-intrusively, and with sufficient resolution, both spatial and temporal, to accurately resolve the turbulent structures of smallest scale. Consequently, the naturally arising question is, "does such a capability already exist, and, if not, is it even possible?"

Various studies have been carried out to determine effective techniques for full-field, simultaneous velocimetry and thermometry. Thermochromic liquid crystals (TLCs) can be used for qualitative visualization of thermofluidic flows [7]. The color reflections of the TLCs when illuminated with white light provide thermometry and the TLCs, if microencapsulated, could serve as tracer particles for PIV. However, TLCs are limited in their useful temperature range (~10°C) and complex in situ calibration is required.

More recently, luminescent temperature-sensitive particles were utilized as PIV tracers for simultaneous velocimetry and thermometry in a heated oil flow [11]. Particles with a mean diameter of 15 μm were dyed with the luminescent molecule Europium (III) Thenoyltrifluoroacetonate and used as tracer particles in a simple thermofluidic flow. Temperature analysis was performed using lifetime measurements, which relies on pulsed excitation light. While this lifetime measurement technique was successful for flow

visualization in this relatively simple flow, this technique is not suitable for complex turbulent flows due to technological and temporal constraints.

Although a solid foundation for simultaneous thermometry and velocimetry for thermofluidic flows has been laid, substantial room for improvement exists and further development of experimental techniques demands pursuit.

Chapter 2. THEORY

The majority of previous applications and research involving temperature-sensitive paint have been in relation to surface measurements, in which the luminescent molecules were immobilized in a polymer-based surface paint. While surface employment can provide very important thermal information for a body in a flow, often times temperature data throughout the flow itself is of greater import and value. Accordingly, a means of utilizing temperature-sensitive paint for flow field thermometry is highly desirable.

Temperature-sensitive beads (TSBs) are capable of meeting this demand. TSBs are small particles, often of silica or polystyrene, that have been doped with a temperature-sensitive luminescent dye. Since the TSBs are not immobilized in an oxygen-impermeable layer, as is the case with most temperature-sensitive surface paints, special care must be taken to ensure that the luminescent dye in use is unaffected by oxygen quenching. Rhodamine, europium, and zinc derivatives have been widely investigated as viable luminescent dyes. Fundamentally, a TSB is merely a particle doped with a temperature-sensitive luminescent dye. However, with turbulent flow visualization in mind, additional requirements must be met for the feasibility of utilizing specific TSBs for simultaneous velocimetry and thermometry.

2.1 PARTICLE SIZE

A number of considerations must be taken when selecting the size of TSBs. Generally, TSBs are on the order of 10 μm, with all TSBs in current literature under 100 μm. The primary reason for the microscopic size of TSBs is spatial resolution constraints. In order for a turbulent flow to be fully resolved, turbulent flow theory dictates that the eddies of smallest scale must be resolved. The Kolmogorov microscales can be used to calculate the turbulent length scale based on kinematic viscosity, ν, and the mean rate of viscous dissipation of the mean kinetic energy per unit mass, ε. Using the Kolmogorov length scale equation,

$$\eta = \left(\frac{\nu^3}{\varepsilon}\right)^{1/4}, \tag{2.1}$$

for an example water flow with turbulent Reynolds number $Re_T = 10^4$ and length scale $l_T = 10^{-2}$ m, the Kolmogorov length scale is $\eta = 10$ μm. Therefore, for the example conditions

above, the TSBs would need to have a diameter smaller than 10 μm to allow for full resolution of the smallest eddies.

2.2 Particle Response Time

PIV relies comprehensively on the assumption that tracer particles follow the same motion as fluid particles in the flow. Hence, determining whether this is the case is imperative. In general, the Stokes number, which is a dimensionless parameter that is a ratio of particle stopping distance to a characteristic length scale of the flow, is the important criterion. For accurate particle tracing,

$$St = \frac{\tau_p * U_\infty}{l} \ll 1, \tag{2.2}$$

where τ_p is the particle relaxation time, U_∞ is the freestream flow velocity, and l is the characteristic length scale. Maximum temporal resolution requires that the relaxation time of the TSBs be faster than the smallest time scale of the flow. Looking again to the Kolmogorov microscales, the Kolmogorov time scale equation is

$$\tau_\eta = \left(\frac{\nu}{\varepsilon}\right)^{1/2}. \tag{2.3}$$

For the same example conditions previously used (water, $Re_T = 10^4$, $l_T = 10^{-2}$ m), the Kolmogorov time scale is $\tau_\eta \approx 100$ μs. The particle relaxation time can be calculated using the equation

$$\tau_p = \frac{(\rho_p - \rho_f) {d_p}^2}{18 \mu_f \phi}, \tag{2.4}$$

where d_p is the particle diameter, ρ_p is particle density, ρ_f is the fluid density, μ_f is the fluid dynamic viscosity, and the function $\phi > 1$ depends on the particle Reynolds number [12]. Accordingly, TSB material and size as well as specific flow conditions must be carefully considered to ensure accurate particle tracing.

2.3 Dye Response Time

In addition to a TSB being capable of quick response to velocity fluctuations, a TSB must be able to rapidly respond to temperature fluctuations. Yet again, the Kolmogorov microscales must be considered. Within a turbulent flow, the smallest eddies are the mechanism for the

molecular diffusion of heat, and therefore, the determining factor for the temperature field. For that reason the dye response time, τ_d, must be faster than the Kolmogorov time scale to enable full temporal resolution for temperature changes. In thermometry, the response time of a temperature sensor is defined as the time required to reach 63.2% of an instantaneous temperature change.

2.4 Particle Density

While particle density is a significant parameter in the determination of particle relaxation time, the density of TSBs is also of import in relation to buoyancy. In the case of gaseous flow problems, TSB density is far greater than the fluid and TSBs will not remain suspended for very long. However, this obstacle is overcome by testing at high speeds for short periods of time and by constantly injecting TSBs into the flow. For the case of liquid flows, where the velocity is lower, concerted effort should be made to select a TSB material that allows for nearly neutral buoyancy.

2.5 Temperature Sensitivity

There are a few desirable traits for a luminescent dye with regards to temperature sensitivity. First, the dye should luminesce in a predictable manner throughout the anticipated temperature range. This condition allows for temperature to be measured quantitatively rather than merely qualitatively, and a linear temperature sensitivity is common and useful. Second, the dye needs to have adequate temperature sensitivity so that relatively small changes in temperature can be detected. Temperature resolution relies entirely on the ability of a dye to change luminescence with measurable magnitude.

2.6 Reference Dye

A number of variables affect the intensity of luminescence. Non-uniformities in particle size and dye saturation as well as non-uniform excitation light can significantly alter luminescent intensity. These variations create a potential for large errors in TSB thermometry. However, the use of a luminescent reference dye is a proposed solution. A second luminescent dye that is insensitive to temperature changes can be incorporated into TSBs. Using optical filtering, the signals of the two dyes are simultaneously measured. By calibrating the TSBs at known constant

temperatures, the effects of non-uniformities can be counteracted. In order to be able to isolate the luminescence of each of the two dyes, it is important that the dyes have spectrally separated emissions.

Clearly, the fidelity of simultaneous velocimetry and thermometry using TSBs is contingent on the characteristics of the particles themselves. Great effort and care must be devoted to the selection of particle material, particle size, and luminescent dyes.

Chapter 3. TEMPERATURE-SENSITIVE DYE ANALYSIS

In the development of temperature-sensitive beads for simultaneous thermometry and velocimetry, due diligence must be given to the task of choosing an optimal dye. The two preliminary measures of merit for dye selection are luminescent intensity and temperature sensitivity. Intuitively, the desired traits are strong luminescence as well as high temperature sensitivity throughout the entire temperature range of interest (~20-45°C). Of additional interest are the excitation wavelength and emission wavelength for a given dye.

A wide assortment of luminescent dyes was selected for further analysis. Luminescent molecules tested include Europium (III) thenoyltrifluoroacetonate (EuTTA), Zinc cadmium sulfide, Terbium-doped gadolinium oxysulphide (Gd_2O_2S:Tb), and Europium-doped lanthanum oxysulphide (La_2O_2S:Eu). A full list of luminescent dyes investigated is shown in Table 3.1.

3.1 EMISSION SPECTRA

Luminescent intensity and emission spectra were measured using an Ocean Optics USB 4000 spectrometer. A sharp peak, as shown in Figure 3.1, is a desirable spectral characteristic. A 375 nm light emitting diode (LED) was used as the excitation light source. The peak emission wavelength of each sample tested can be found in Table 3.1.

3.2 TEMPERATURE SENSITIVITY

Temperature sensitivity analysis was performed using a photomultiplier tube (PMT) apparatus. The apparatus consists of a light source, mirror, optical lenses, test chamber, PMT, optical filters, and a data acquisition system (DAS). A schematic for the apparatus is shown in Figure 3.2. The test chamber, which houses luminescent test samples, is capable of changing the test chamber pressure below atmospheric and altering the test sample temperature. Pressure sweeps at constant temperature were run for each luminescent sample to ensure that luminescent intensity was insensitive to pressure change. For all dyes tested, pressure sensitivity was found to be negligible.

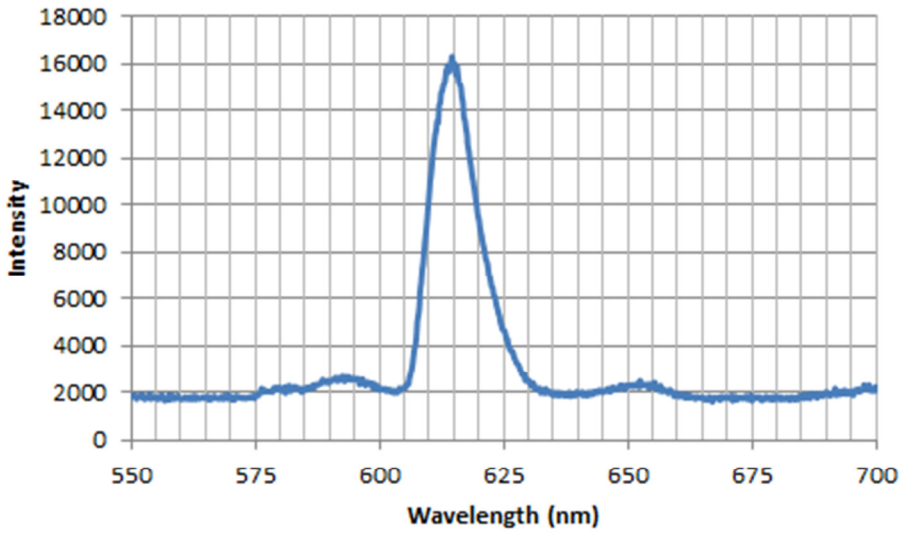

Figure 3.1 Spectral emission for EuTTA, excited with 375 nm LED

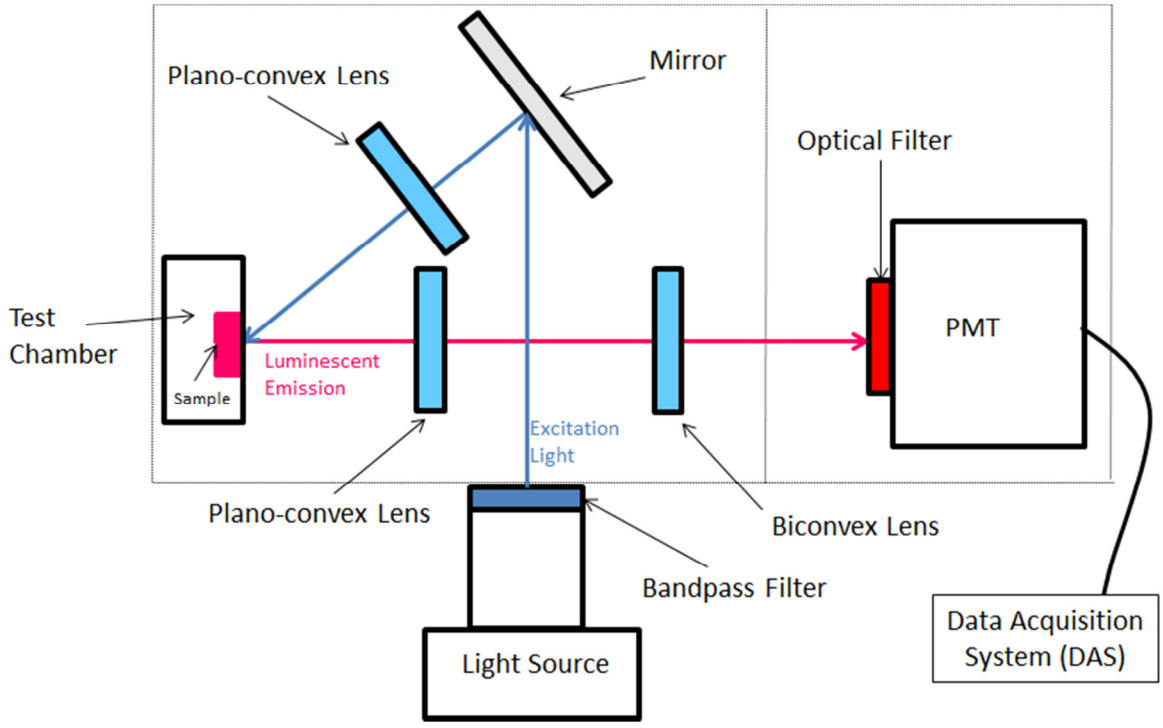

Figure 3.2 Photomultiplier tube apparatus

Temperature sweeps at ambient pressure (~760 mm Hg) were also run for each luminescent sample to determine temperature sensitivity, with a temperature range from 5-45 °C. Results from the temperature sensitivity analysis are displayed in Table 3.1.

Table 3.1 Summary of luminescent dye analysis

Luminescent Dye	Peak Emission Wavelength (λ_{max}) nm	Temperature Sensitivity % ΔI/°C
EuTTA	615	-1.94
ZnCdS 3251	550	-1.14
YagTb	545	-0.13
Y_2O_3Eu	610	-0.11
Sylvania 250	510	0
ZnS:Cu 3003	535	0.01
Gd_2O_2S:Tb	545	0.24
YVO_4:Eu	615	1.18
La_2O_2S:Eu	540 / 620	-0.23 / 0.17

3.3 RESULTS

Table 3.1 summarizes the dye analysis results for the luminescent dyes tested, shown in ascending order for temperature sensitivity. The luminescent molecule showing the temperature sensitivity of greatest magnitude of 1.94% change in intensity per °C was EuTTA (Figure 3.3).

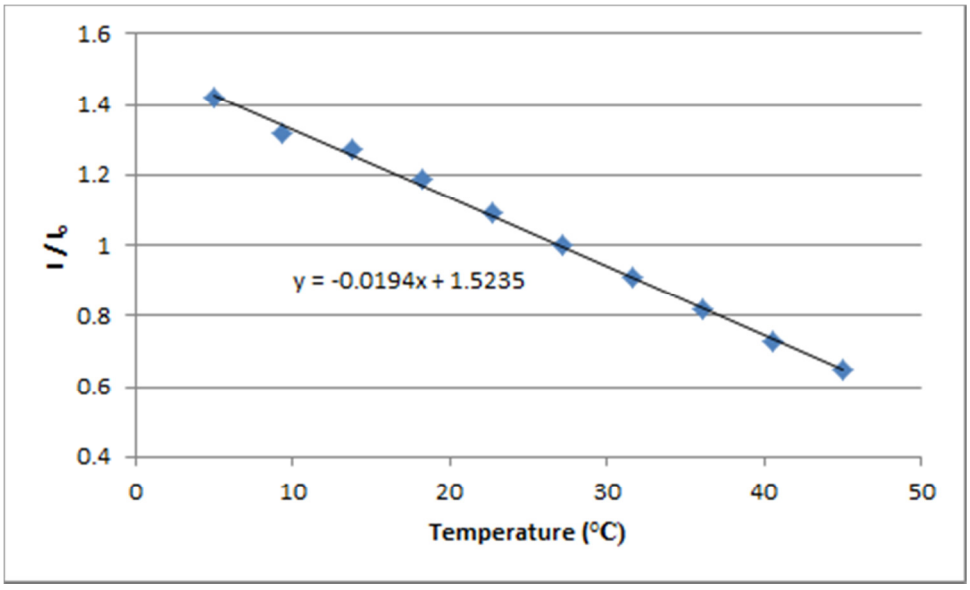

Figure 3.3 Temperature sensitivity for EuTTA

Zinc cadmium sulfide (ZnCdS) and Europium-doped yttrium vanadate (YVO_4:Eu) also displayed temperature sensitivities with magnitude greater than 1% ΔI/°C and strong luminescence. The temperature sensitivities for ZnCdS and YVO_4:Eu are shown in Figures 3.4

and 3.5, respectively. While the figures clearly show that a polynomial regression would more accurately model the temperature trend, both plots have been fitted with linear regressions for a better comparison to other dyes.

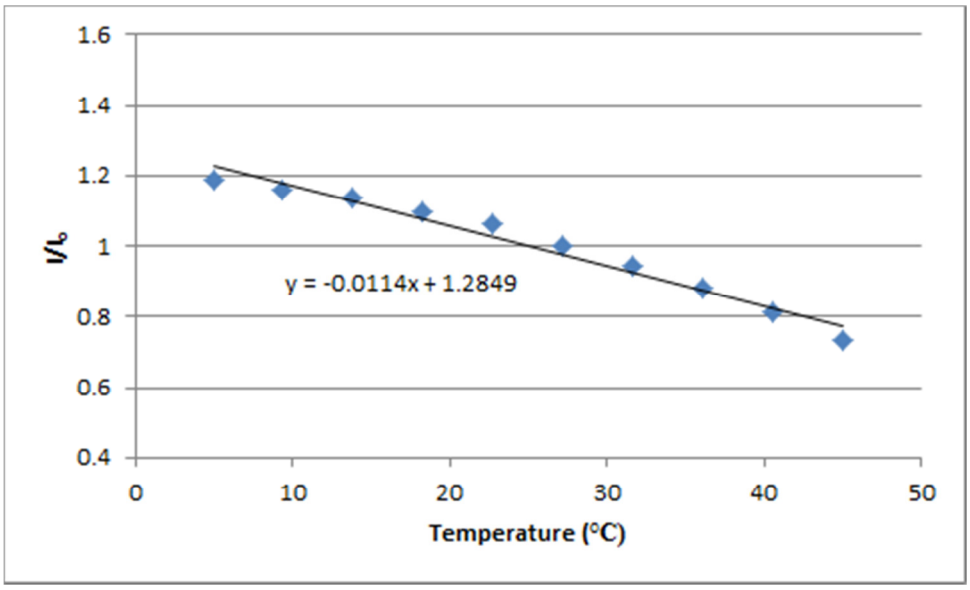

Figure 3.4 Temperature sensitivity for ZnCdS

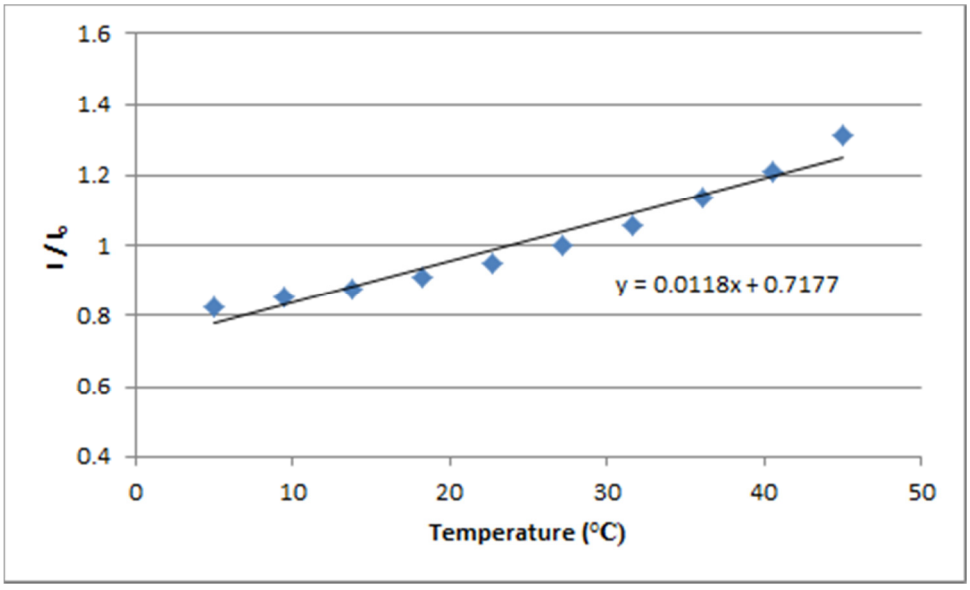

Figure 3.5 Temperature sensitivity for YVO_4:Eu

Another notable feature of Table 3.1 is the peak emissions and sensitivities for La_2O_2S:Eu. La_2O_2S:Eu showed an emission spectrum with two distinct peaks at 540 nm and 620 nm. Bandpass filters corresponding to these wavelengths were used to isolate the temperature sensitivities of these peaks individually. The peak at 540 nm showed a negative temperature sensitivity of 0.23% ΔI/°C and the peak at 620 nm exhibited a positive temperature sensitivity of 0.34% ΔI/°C. Although the magnitudes of these sensitivities are small, the opposite responses of these peaks could potentially be combined to arrive at a new temperature sensitivity of greater magnitude. However, the expected magnitude of this new sensitivity would essentially be the difference of the two temperature sensitivities, approximately 0.5% ΔI/°C.

Upon completion of spectral and thermal sensitivity analysis, EuTTA was selected as the best candidate for further testing, including a time response investigation and TSB development. This determination was made based on the luminescent molecules' substantial temperature sensitivity. High thermal resolution is greatly desired for optimal TSBs, and EuTTA affords the best opportunity to achieve this outcome.

Chapter 4. DYE RESPONSE TIME

In order to perform accurate thermometry with TSBs in a turbulent flow, the temperature-sensitive luminescent dye must be capable of responding to temperature changes very quickly. As discussed previously, this temporal resolution criterion can be met by ensuring that the dye response time is less than the Kolmogorov time scale. While the calculation of the requisite response time is quite simple, its measurement is quite challenging.

4.1 MEASUREMENT SYSTEM REQUIREMENTS

A few requirements exist for a measurement system to be capable of measuring the response time of a luminescent dye. Since the response time is defined as the time to reach 63.2% of an instantaneous temperature change, a fundamental prerequisite for response time measurement is a means of imparting an instantaneous or step temperature change. Imparting a step temperature change is simple in theory, but quite difficult in practice. A few methods for doing so are discussed in following sections.

An additional requirement for accurately determining response time is a sensor to measure how the luminescence of the temperature-sensitive dye changes due to the temperature change. Underlying this requirement are two sensor requirements: high sensitivity and high temporal resolution. Changes in the intensity of luminescence with respect to temperature change are small, as seen with the ~2% ΔI / °C temperature sensitivity for EuTTA. Unless an exceptionally large temperature change can be imparted, a small change in luminescence is expected and a sensor with high sensitivity is needed to detect an intensity variation of respectively low magnitude. Furthermore, to measure response times that could potentially fall in the sub-millisecond regime, a sensor with high temporal resolution must be used.

4.2 SHOCK TUBE

Normal shock relations dictate how fluid properties vary in flows with stationary or propagating normal shock waves. Across a shock wave, pressure, density, and temperature change in a stepwise manner. Specifically, the temperature jump across a normal shock in a perfect gas can be related to shock number by the equation

$$\frac{T_2}{T_1} = 1 + \frac{2(\gamma - 1)}{(\gamma + 1)^2}\frac{\gamma {M_1}^2 + 1}{{M_1}^2}\left({M_1}^2 - 1\right), \tag{4.1}$$

where T_2 is static temperature after the shock, T_1 is static temperature before the shock, γ is the ratio of specific heats for the gas, and M_1 is the Mach number of the shock [13]. Property variation due to a normal shock occurs over such a small distance (shock thickness) and at such a high speed (shock velocity) that the corresponding "shock time" is extremely small and the temperature change can be considered instantaneous. Consequently, a shock wave is one mechanism for imparting a step temperature change.

A shock tube is an experimental apparatus for creating and effectively utilizing normal shock waves. The apparatus consists of two chambers, a driver and a driven chamber, separated by a diaphragm. A pressure difference between the chambers is created by pressurizing or depressurizing one chamber, or by means of a chemical reaction. The pressure difference increases until the diaphragm bursts, at which point a shock wave propagates into the driven chamber and an expansion wave propagates into the driver chamber. As the shock front passes through the driven chamber, the fluid properties in the chamber change in accordance with the normal shock relations.

A shock tube constructed by Kimura was used for response time testing [14]. The shock tube is fashioned from 5 cm square aluminum tubing with an inner cross-sectional area of 3.9 x 3.9 cm^2. The driving section is 3.1 m long and the driven section is 1.8 m long. Parafilm® *M* (127 μm thickness, Pechiney Plastic Packaging, Measha, WI) serves as the diaphragm material and is burst by the pressure difference between the driver and driven sections. The pressure difference is achieved by lowering the pressure in the driven section with a vacuum pump. The shock tube is non-chemically reacting and the working fluid is air. The shock strength can be varied by increasing or decreasing the number of Parafilm layers used. A 1.9 x 3.8 cm^2 test window made of polycarbonate is positioned 0.58 m downstream of the diaphragm. Dynamic pressure is measured 0.64 m downstream of the diaphragm, 0.12 m past the location of the test samples. Absolute pressure is measured at the end wall of the driven section. The schematic of the shock tube is shown in Figure 4.1.

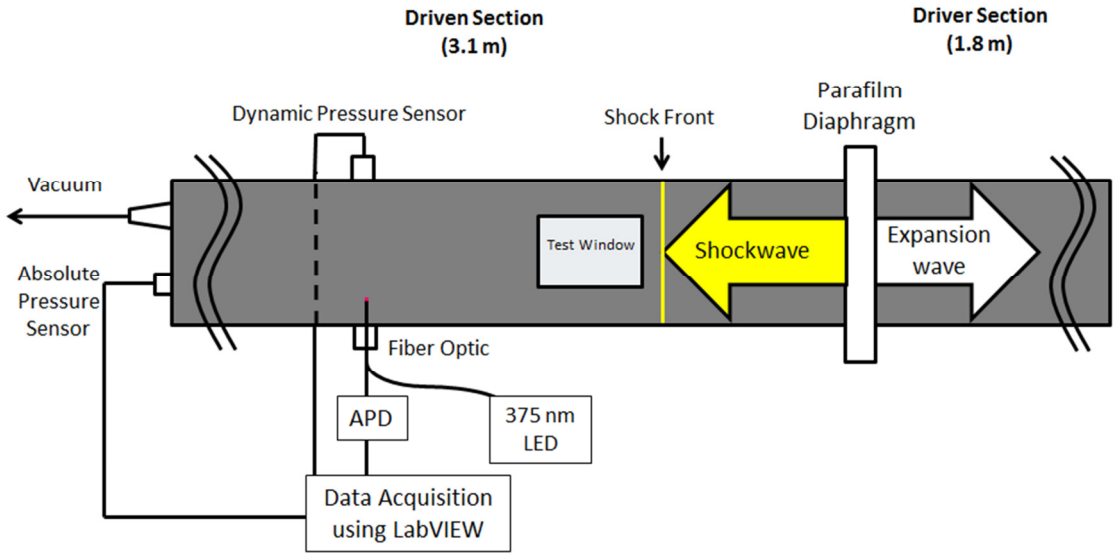

Figure 4.1 Schematic of shock tube with fiber optic setup

4.2.1 *Photomultiplier*

The first sensor used to measure the luminescence of temperature-sensitive dyes in the shock tube was a Hamamatsu R928 photomultiplier tube. The PMT has a 2.2 ns rise time and a gain of $1.0x10^7$ for an applied voltage of 1000 V. EuTTA with Max polymer was applied to a micro cover glass slide, which was then mounted inside the shock tube flush with the test window. The luminescent sample was oriented to face the center of the tube, as opposed to in contact with the window, to allow for better heat absorption from the shock wave. A 375 nm LED was used to illuminate the dye. A pair of optical lenses was used to focus the luminescent emission onto the PMT, which was fitted with a 610 nm bandpass filter to filter out light from the LED and other sources while allowing the EuTTA luminescence to be detected. Data for the pressure transducers and PMT was acquired using a National Instruments NI USB-6251 data acquisition board in concert with LABVIEW Signal Express, sampling at 100 ks/s.

Shock tube testing with the PMT as a detector proved unsuccessful for measuring the thermal time response. The shock Mach number and temperature ratio can be calculated from pressure data and shock tube dimensions. For a driven pressure of 68.8 kPa and a driver pressure of 100 kPa (achieved using a 2-ply diaphragm), the shock wave propagates at $M = 1.08$, and the temperature ratio is $\frac{T_2}{T_1} = 1.052$. The temperature change experienced is approximately 15°C. Since EuTTA has a temperature sensitivity of ~2% ΔI/°C, a 30% change in intensity would be

expected. While pressure data clearly showed the pressure jump across the shock, no observable change in the intensity of luminescence was seen in the PMT data.

Additional testing was performed in the shock tube with the test sample at a different location. The center of the tube (~2 cm from the wall) would be an ideal location for the sample in order to be at the center of the shock wave. However, spatial and mechanical limitations of the shock tube led to placement of the glass slide 1 cm from the tube wall, oriented parallel to the flow. Once more, shock tube testing with the PMT did not show any visible temperature response.

There are various factors that contribute to the inability to measure response time with the PMT. For the setup with the luminescent sample placed on the test window, thermal insulation is a concern. As a result of the sample's proximity to the highly thermally conductive aluminum walls, the sample is not insulated from the outside environment. Heat loss to the environment can significantly decrease the temperature change experienced by a sample on the test window compared to a sample located in the middle of the flow, as was shown in a study by Kimura [15]. Another concern is that the sample may lie within the tube wall boundary layer. While pressure changes would readily be experienced by the sample since pressure acts normal to the flow, temperature changes would not necessarily be undergone, as temperature more freely propagates in the direction of the flow.

For the setup with the luminescent sample extended into the flow, 1 cm from the tube wall, the thermal insulation and tube wall boundary layer concerns were effectively eliminated. However, the slide location generates a new concern regarding the creation of a bow shock at the leading edge. As the shock passes over the slide, a bow shock is created at the upstream edge, likely preventing the luminescent sample from experiencing an instantaneous temperature change.

Overall, for both setups the combination of a weak excitation source, a low intensity emission due to small sample size, and considerable shot noise makes for a rather poor signal-to-noise ratio that could have largely obscured the detection of an intensity change with the passing of the shock. As a preliminary luminescent sensor, the PMT was ineffective in detecting the intensity changes desired for determining the thermal response time of EuTTA.

4.2.2 *Fiber Optic with Avalanche Photodiode (APD)*

A novel setup for improving the influence of the shock wave on the luminescent sample was conceived. This setup, shown in Figure 4.1, employs a thin optical fiber extended into the shock tube. The tip of the optical fiber is painted with a very small amount of luminescent dye and the dye is excited by a 375 nm LED illuminating the fiber. By extending the fiber away from the shock tube wall and into the flow, less heat should be lost to the outside environment.

Since the amount of luminescent dye is smaller and the excitation source is once again weak, a different luminescence sensor is required. A Hamamatsu C5460 avalanche photodiode (APD) with a fiber optic adapter was used. The APD has 10 MHz bandwidth and a minimum light detection limit of 0.8 nW, providing the requisite speed and sensitivity.

The response time for EuTTA with Max polymer painted on a 1 mm optical fiber extended 2 cm into the tube is shown in Figure 4.2. Plotted in blue is the continuous APD voltage data recorded at 100 kHz and in yellow is a filtered response curve found via a regression using weighted linear least squares with a 2nd degree polynomial. As the shock wave passes the luminescent sample the temperature increases, leading to a decrease in luminescence/voltage, as the plot clearly shows. The calculated response time is 55 ms.

In order to verify that this measurement is the response time of the dye itself and not merely the response time of the optical fiber, additional testing was undertaken to attempt to measure the temperature rise across the shock using thermocouples.

4.2.3 *Thermocouple Testing*

Three T type thermocouples of varying diameter (400, 100, and 50 µm) were used to characterize the temperature jump across the shock wave in the shock tube. The 400 µm thermocouple was a medical grade, exposed junction sensor and the 100 µm thermocouple was a standard thin wire, exposed junction sensor. The 50 µm thermocouple was an Omega precision fine wire thermocouple. The 400 and 100 µm thermocouples demonstrated response times on the order of tens of milliseconds, while the 50 µm thermocouple displayed response times on the order of milliseconds. The fastest response time of 2.2 ms was measured using the 50 µm thermocouple, and Figure 4.3 shows a plot of the response. The published response time by Omega for a similar thermocouple (type J) is 4 ms, which agrees well with the response time measured in the shock tube.

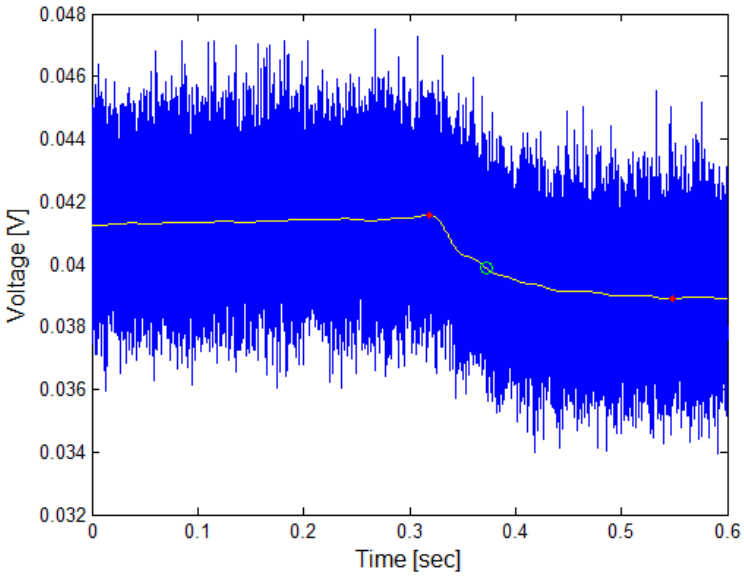

Figure 4.2 Time response from APD voltage for EuTTA

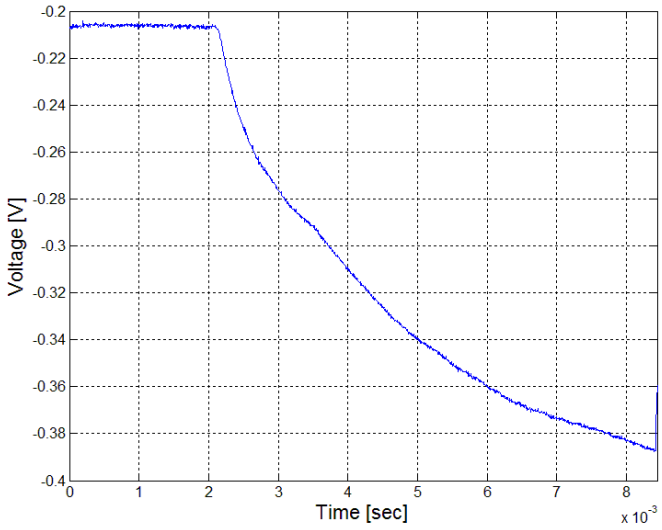

Figure 4.3 Thin wire thermocouple (50 µm) response to shock wave

The overall implications for the thermocouple results are somewhat ambiguous. The fine wire thermocouple was able to respond to the shock wave with a response time of 2.2 ms, while the APD with EuTTA exhibited a response time of 55 ms. The possibility exists that the actual response time of the temperature-sensitive dye is 55 ms. However, the possibility also exists that the APD and fiber optic setup itself is the limiting factor. Accordingly, an alternate means of measuring the response time of EuTTA should be investigated.

4.3 PULSE LASER HEATING

Another method for imparting a step temperature input is through the use of a laser. By pulsing a laser for a short duration, with sufficient power, pulse laser heating can be performed to provide a nearly instantaneous temperature jump. Pulse laser heating was implemented by Liu et al. using a Nd:YAG laser (532 nm at an 800-mJ maximum output) and a PMT to measure a 250 μs response time for Ru(bpy)-Shellac temperature-sensitive paint [16].

Currently, a similar technique has been proposed and is being developed within our research group for pulse laser heating using an infrared laser. The primary advantages of using an infrared laser are increased modulation controllability as well as spectral separation to prevent interaction between the pulse laser and the luminescent emission. Eventually this technique may prove more effective in measuring the response time of luminescent dyes than the current shock tube techniques.

Chapter 5. BEAD FABRICATION

Following temperature sensitivity analysis of various luminescent dyes, bead fabrication efforts were carried out in parallel with time response testing. TSBs were developed at both Washington University in St. Louis (WUSTL) and the University of Washington (UW).

5.1 WUSTL BEAD FABRICATION

Professor Younan Xia and Cun Zhu at WUSTL have iteratively fabricated TSBs for the simultaneous velocimetry and thermometry technique that is the focus of this paper. In the first phase of development, highly uniform polystyrene microspheres doped with EuTTA dye (E dye) were fabricated. The microspheres, shown in Figure 5.1, have a diameter of approximately 2 μm.

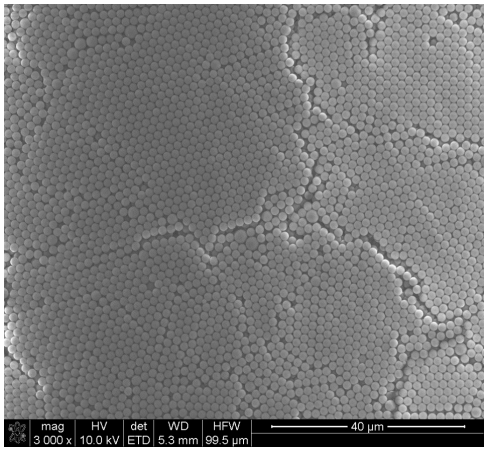

Figure 5.1 Image of polystyrene E dye microspheres from WUSTL

Spectrometry and temperature sensitivity testing of these TSBs confirmed that the spectral and thermal sensitivity properties of EuTTA were not altered by the application of the luminescent dye to the polystyrene particles.

In the subsequent phase of development, a temperature-insensitive luminescent reference dye, Coumarin 500 (H dye), was also incorporated into the TSBs. These TSBs are designated E-H #1. The spectral emission is shown in Figure 5.2. A 375 nm LED is the sole excitation source. The H dye has a fairly broad emission centered on 515 nm and the E dye continues to display a sharp emission at 615 nm. The separation of the two peaks is ideal for isolation of the

two luminescent emissions. Temperature sensitivity testing indicated a negligible 0.2% ΔI/°C for the H dye and an improved 2.35% ΔI/°C for the E dye.

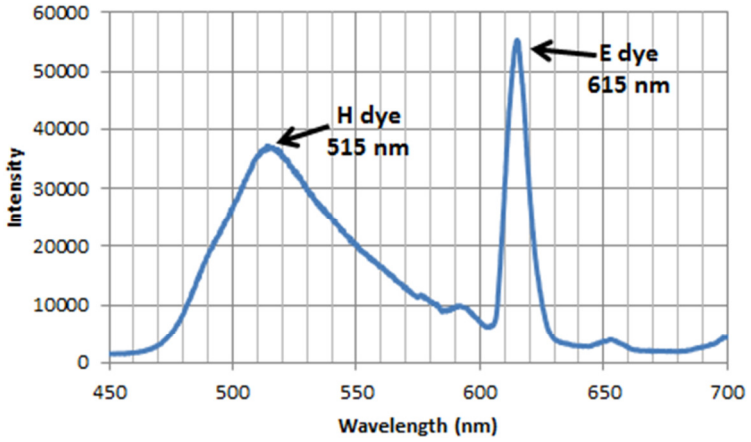

Figure 5.2 Emission spectrum for E-H #1 polystyrene beads

Although the characteristics of the initial E-H #1 TSBs were favorable, the small size of the beads was of concern. For flow visualization at non-microscopic scales, the 2 µm diameter could be too small for PIV. Furthermore, the small bead size results in low luminescence, possibly beyond the detection capabilities of many cameras. Accordingly, new E-H TSBs of larger diameter were requested.

WUSTL was able to fabricate larger E-H beads with approximately 4 µm diameter, designated E-H #2. These particles were less uniform. However, the presence of a reference dye makes non-uniformities in particle size irrelevant. The 4 µm particles are shown in Figure 5.3.

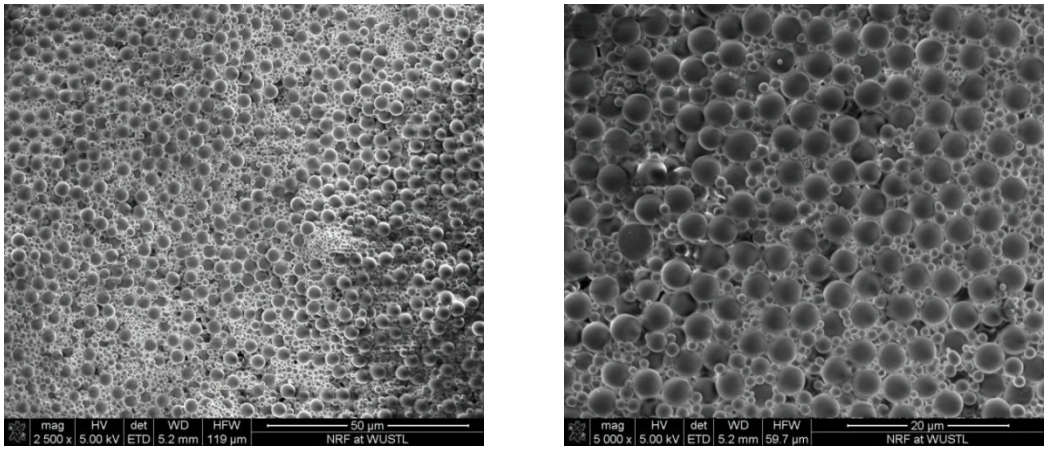

Figure 5.3 Images of polystyrene E-H #2 beads from WUSTL

5.2 UW BEAD FABRICATION

In response to the demand for beads large and bright enough for simultaneous PIV and luminescent thermometry, TSB fabrication efforts were also undertaken at the UW. Two types of beads that have been successfully used at the UW as PIV tracers were selected. One type was Sphericel hollow glass spheres produced by Potters Industries Inc. The glass spheres have a density of 1.10 g/cm^3 and a mean diameter of 13 µm. The second type was Conduct-O-Fil silvered hollows, also produced by Potters Industries Inc. The silvered hollows have a density of 1.6 g/cm^3 and a mean diameter of 13 µm.

E dye beads of each of the two types were fabricated separately, using the same process. 100 mg of EuTTA was combined with 10 mL of Dichloromethane. The solution was mixed using a magnetic stirrer for approximately two hours before adding 1000 mg of glass/silver beads. The new solution was allowed to mix via magnetic stirrer for an additional 20 hours before the solvent was evaporated by first heating the solution on a stirrer hotplate and then further heating the dyed beads in an oven at 75°C. Clumps of beads were manually, mechanically broken into a coarse powder using a metal spatula. Finally, the powder was pulverized using a mortar and pestle. The spectral emission of particles excited by a 375 nm LED showed a strong peak at 615 nm for both glass and silver beads, as expected.

Incorporation of a reference dye was attempted only for the hollow glass spheres due to density considerations. 30 mg of Coumarin 500 was mixed with 250 mg of Sphericel E-dye particles and 4 mL Dichloromethane. Steps similar to those above were taken to produce the E-H hollow glass spheres, designated E-H-UW TSBs.

Chapter 6. NATURAL CONVECTION FLOW VISUALIZATION

Natural convection is a type of heat-driven fluid motion resulting from density differences in a fluid due to temperature gradients. Fluid near a heat source receives heat, leading to decreased density and, thus, rising of the fluid. As the heated fluid rises, surrounding cooler fluid moves into the region near the heat source and the process is repeated, creating a buoyant plume. Within the rising plume the flow transitions from laminar to turbulent flow at a distance above the heat source correlating mainly to the Grashof number,

$$Gr = \frac{g\beta(T_s - T_\infty)D^3}{\nu^2}, \tag{6.1}$$

where g is gravitational acceleration, β is the coefficient of thermal expansion, T_s is the surface temperature of the heat source, T_∞ is the ambient temperature of the fluid, D is the diameter of the heat source, and ν is the kinematic viscosity [17]. Since both laminar and turbulent flow regions exist in the buoyant plume, natural convection is an ideal flow for visualization using TSBs.

The experimental setup for natural convection flow visualization consists primarily of a glass tank (27.5 cm long, 22.5 cm tall, 7.5 cm wide) and a circular cylinder cartridge heater (1.9 cm diameter, 12.7 cm length, Omega CSS-505500) spanning the tank width. A 370 nm laser beam is passed through a half-cylinder lens to create a thin laser sheet for TSB excitation, as shown in Figure 6.1. Two high-speed, high-sensitivity cameras (Hamamatsu ImagEM C9100-13) are situated on opposite sides of the tank, each fitted with an optical filter to measure the luminescence of one of the two dyes in the dual-dye TSBs (Figure 6.2).

The tank is filled with water at room temperature (25°C) and TSBs are suspended with a particle number density suitable for PIV. The cartridge heater is powered by a power supply with a max voltage of 130 V. The desired temperature range for the flow is 25-45°C.

Three different TSBs were tested within the water flow. From WUSTL, the two E-H TSBs with mean diameter 2 μm and 4μm were tested, as well as the E-H-UW TSBs with a mean diameter of 13 μm.

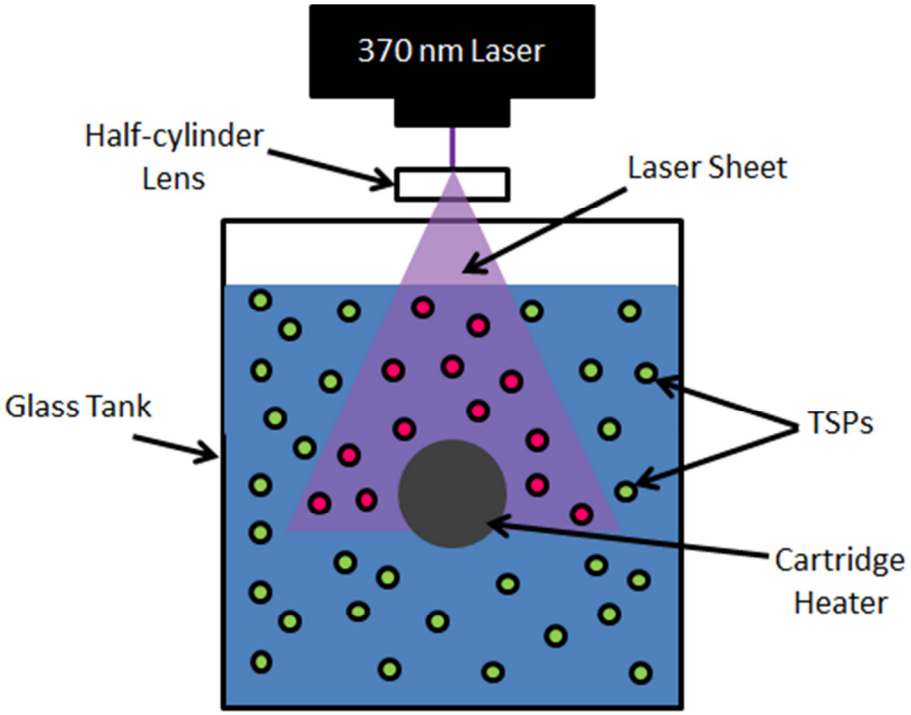

Figure 6.1 Experimental setup from view of camera

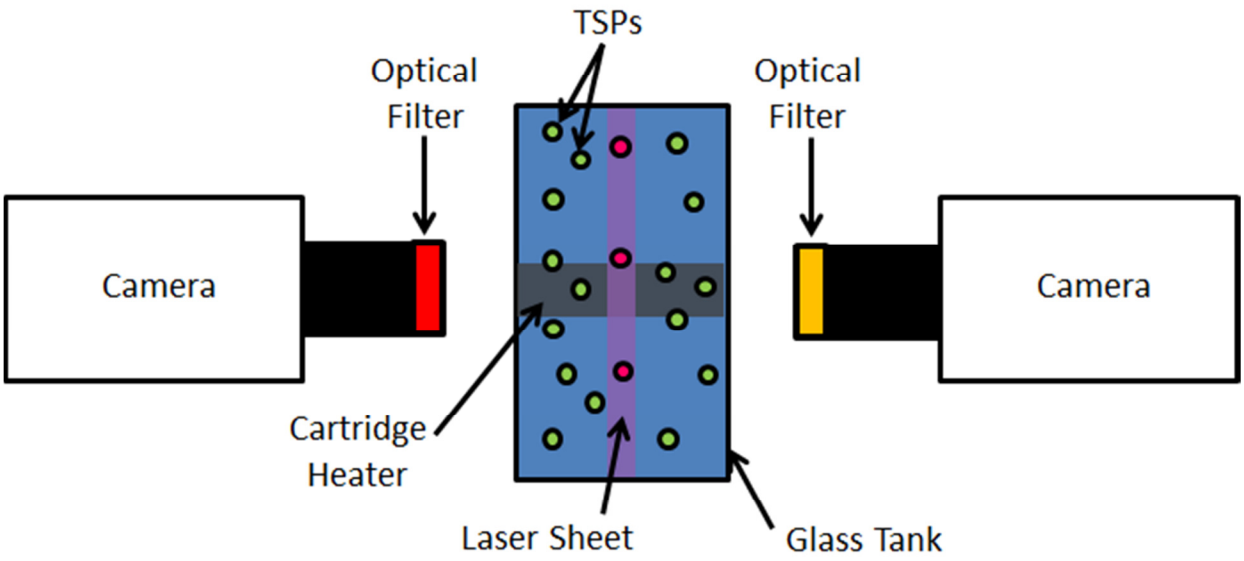

Figure 6.2 Experimental setup from top view (laser and lens omitted)

Chapter 7. RESULTS

For the investigation of natural convection in water for a 25-45°C temperature range, the Grashof number is $Gr = 6.0\text{E}6$. This translates to a Rayleigh number of $Ra = 4.0\text{E}7$. Using an effective Reynolds number formula derived for natural convective boundary flows, where $Re_E = Gr^{\frac{1}{2}}$, the corresponding effective Reynolds number is 2.4E3 [18]. Kolmogorov microscale calculations yield a length scale $\eta = 47$ µm and a time scale $\tau_\eta = 2.5$ ms.

Testing with the E-H #1 TSBs revealed that the 2 µm particles did not exhibit sufficient luminescence. Although the TSBs were bright enough to be seen with the naked eye, neither the E dye peak nor the H dye peak was adequately detectable with the high-sensitivity cameras when appropriate filters were used. The E-H #1 TSBs are not satisfactory for thermometry with the aforementioned setup, although they could potentially still be used as PIV tracers.

Testing with the E-H #2 TSBs showed that the increased luminescent signal of the 4 µm particles was a noteworthy improvement upon the E-H #1 TSBs. While the E dye peak remained visible to the camera with the applicable optical filter, the H dye peak was not strong enough to be visible with filtering. As a result, the E-H #2 TSBs could possibly be used for low-accuracy thermometry since they lack the capability of counteracting particle and lighting non-uniformities that the reference dye enables. Similar to the E-H #1 TSBs, the E-H #2 TSBs could be used as PIV tracers.

The 13 µm E-H-UW TSBs were tested with results comparable to the E-H #1 TSBs. Neither the E dye nor the H dye peaks were detectable with optical filtering. Despite the expected luminescent advantage due to the larger size of the particles, the fabrication process was not effective in creating TSBs with sufficient luminescence. The hollow glass spheres have been used in previous studies as PIV tracers and could be utilized with luminescent dye for improved visibility.

Following the testing of the E-H #1, E-H #2, and E-H-UW TSBs, a request was submitted to WUSTL for the fabrication of new E-H beads with stronger luminescent signals for both dyes. WUSTL produced these new beads, designated E-H #3 TSBs. The beads have a slightly increased diameter of 5 µm and images of the particles are shown in Figure 7.1.

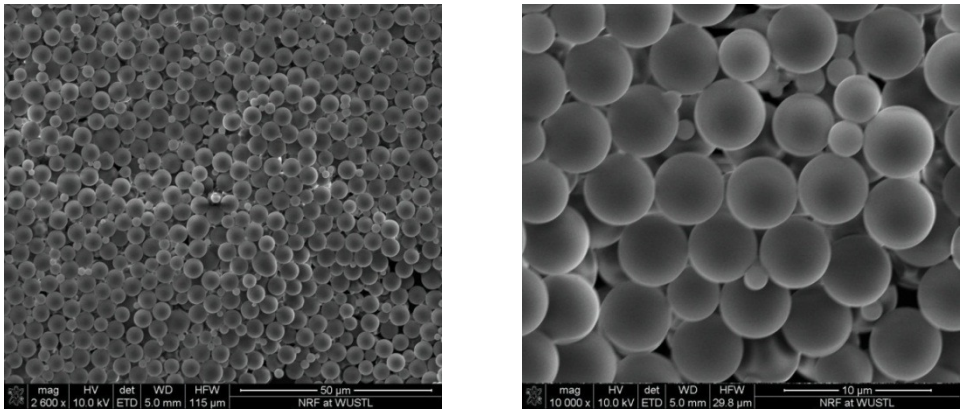

Figure 7.1 Images of polystyrene E-H #3 beads from WUSTL

Testing of the E-H #3 TSBs showed remarkably strong luminescence. Both the E dye and H dye peaks were very visible with optical filtering even at low gain camera settings. The E-H #3 TSBs have a particle relaxation time $\tau_p \leq 144$ ns, allowing for accurate particle tracing. Also, the 5 µm particle diameter is well below the Kolmogorov length scale ($\eta = 47$ µm) for the aforementioned test conditions. Furthermore, the polystyrene TSBs have a density $\rho_p = 1050$ kg/m^3, allowing for nearly neutral buoyancy in water ($\rho_f \approx 1000$ kg/m^3). To date, a thermal response time has not been measured for the E-H #3 TSBs. Efforts to develop the technique of pulse infrared laser heating are currently in progress with this measurement in mind.

The E-H #3 TSBs showed promising results for natural convection flow visualization. The luminescent TSBs made the buoyant plume clearly visible, even to the naked eye. An image with an exposure time of 30 ms is shown in Figure 7.2. The field of view (FOV) for the image is directly above the circular cylinder heater, with the heater just below the image. The luminescence for Figure 7.2 is solely from the temperature-sensitive E dye, with the colorbars beneath providing a qualitative scale for temperature within the flow. It should be noted that hotter temperatures fall on the left end of the colorbar (darker color) and cooler temperatures fall on the right end (lighter color) since luminescence decreases as temperature increases for E dye. The hottest region of the buoyant plume occurs near the middle of the image, rising vertically, and is evident from the dimming of TSBs in this area.

Figure 7.3 shows a plot of PIV results for the image in Figure 7.2 and a consecutive image. The velocity vectors show the vertical motion of rising heated fluid and also demonstrate that the flow immediately above the heated circular cylinder is laminar.

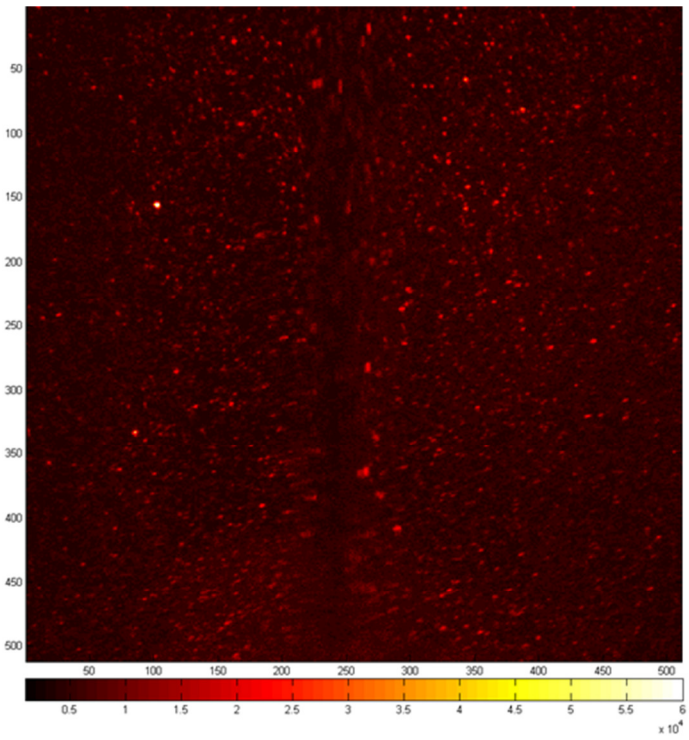

Figure 7.2 E-H #3 TSB natural convection flow visualization (low FOV)

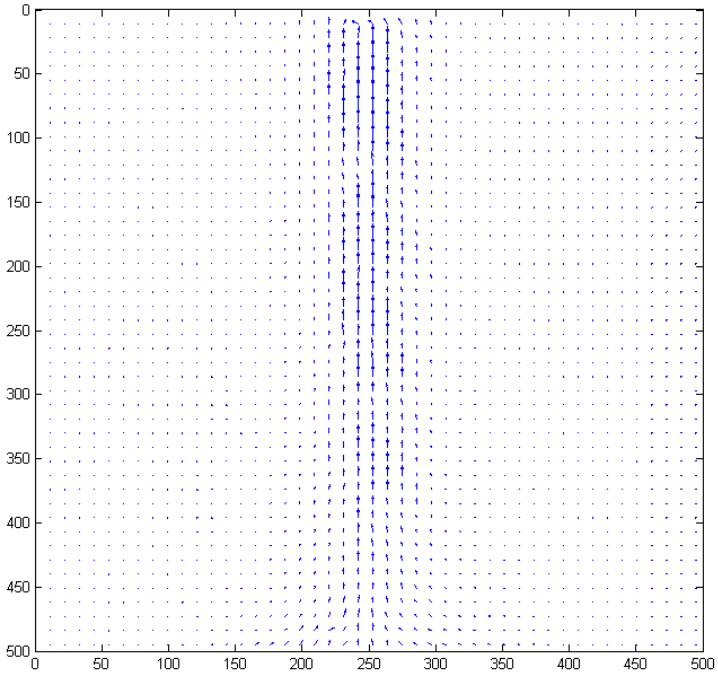

Figure 7.3 E-H #3 TSB natural convection PIV (low FOV)

Figure 7.4 shows an image of the same flow with the FOV located directly above the heater approximately 60 mm. At this height in the flow, transition has begun and turbulent structures are being produced. The flow is no longer as ordered as the low FOV. In general, the TSBs have greater luminescence in this region, meaning that the temperature is lower for this high FOV than for the low FOV. Figure 7.5 shows a plot of PIV results for the high FOV. The velocity vectors show the curving motion of the heated core as vortex shedding occurs. Additionally, large eddies are evident in the PIV plot, but distinguishing them is somewhat difficult due to relatively low-magnitude vorticity. Higher turbulent definition can be observed in real-time or within videos of consecutive image.

One feature that is evident in the images of both FOVs is particle streaking, resulting from the exposure time of images. The exposure time of 30 ms for the images presented leads to lower accuracy PIV due to the velocity gradients existing for the given test conditions. 30 ms is the fastest exposure time of which the ImagEM camera is capable. Accordingly, a high-speed camera with faster imaging capabilities is needed to perform PIV with temporal resolution in alignment with the Kolmogorov time scale $\tau_\eta = 2.5$ ms.

A temperature calibration for the E-H #3 TSBs was performed using a static sample of nebulizer-deposited beads. The temperature of the sample was varied from 25-50°C and images of each dye were taken at 5ºC increments. A calibration curve was created by taking a ratio of the two dye intensities at a given temperature over a small, uniform region of interest (ROI). The resulting temperature sensitivity, as measured with a Hamamatsu ImagEM camera, is shown in Figure 7.6. The calibration showed a temperature sensitivity of approximately 1% change in intensity ratio per °C.

Subsequently, the temperature calibration was applied to images to make the progression from qualitative thermometry to quantitative thermometry. Figure 7.7 shows simultaneous images of the TSBs for the E dye and for the H dye. The FOV was positioned such that the buoyant plume is situated at the left side of the images, evidenced by the PIV vector field plotted in Figure 7.8. Due to alignment inconsistencies between the two cameras, pixel to pixel intensity ratio analysis was not possible. Accordingly, intensity values for each image were first averaged over 64 x 64 pixel windows, with 50% overlap. Then, window to window ratios of the images were taken to create an intensity ratio map, to which the temperature calibration was applied to generate a temperature map. These maps are shown in Figure 7.9.

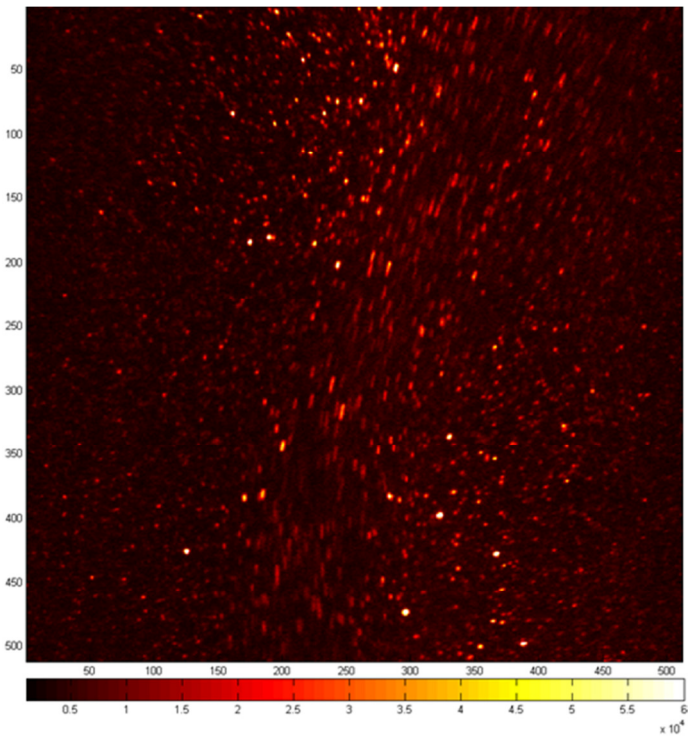

Figure 7.4 E-H #3 TSB natural convection flow visualization (high FOV)

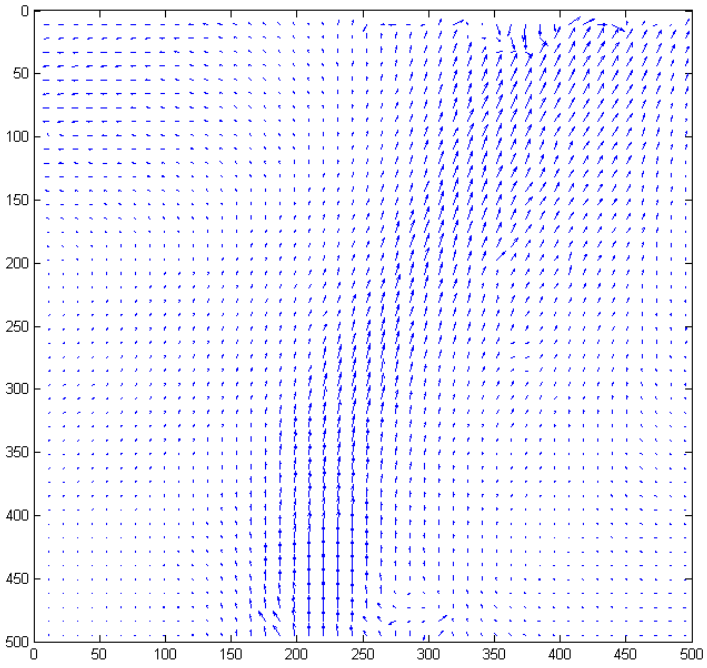

Figure 7.5 E-H #3 TSB natural convection PIV (high FOV)

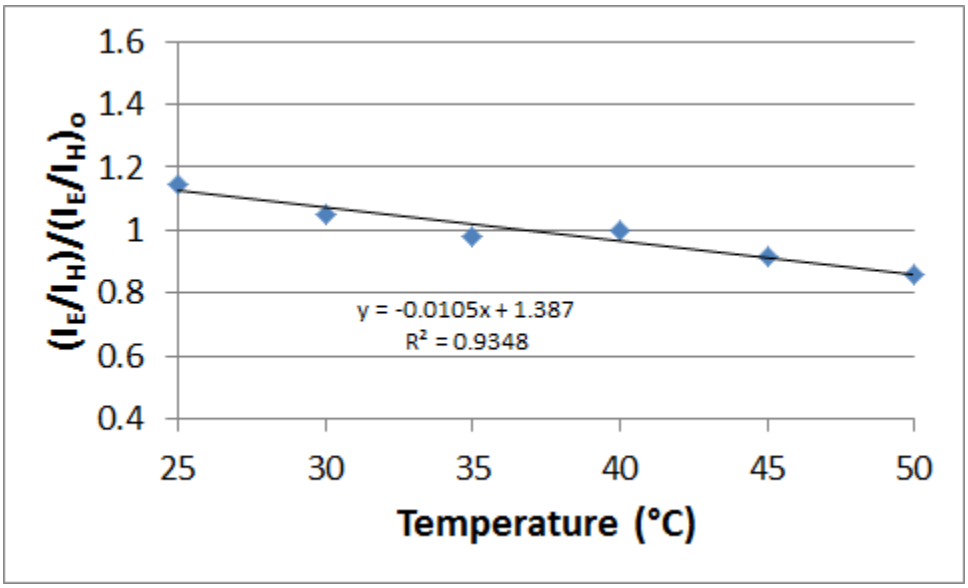

Figure 7.6 Temperature sensitivity for E-H #3 TSBs

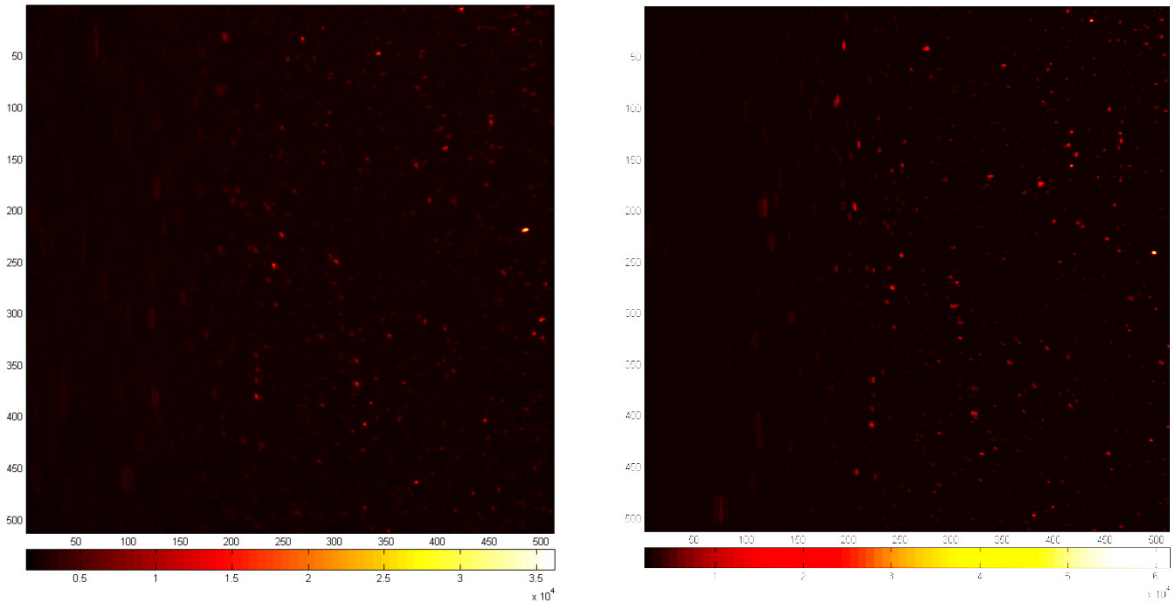

Figure 7.7 E-H #3 TSBs, E dye (left) and H dye (right)

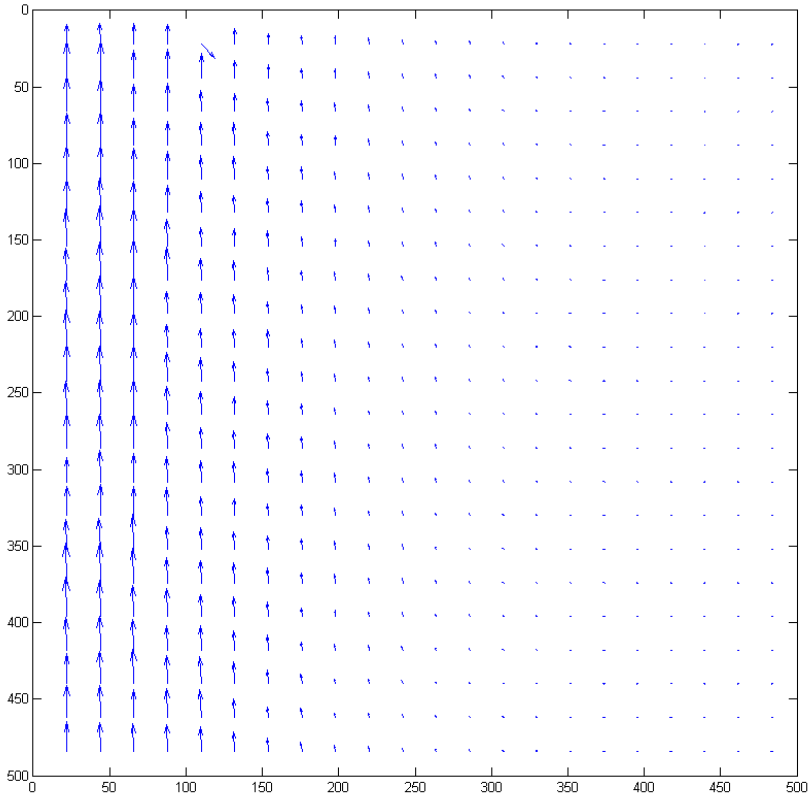

Figure 7.8 E-H #3 TSB natural convection PIV (plume at left)

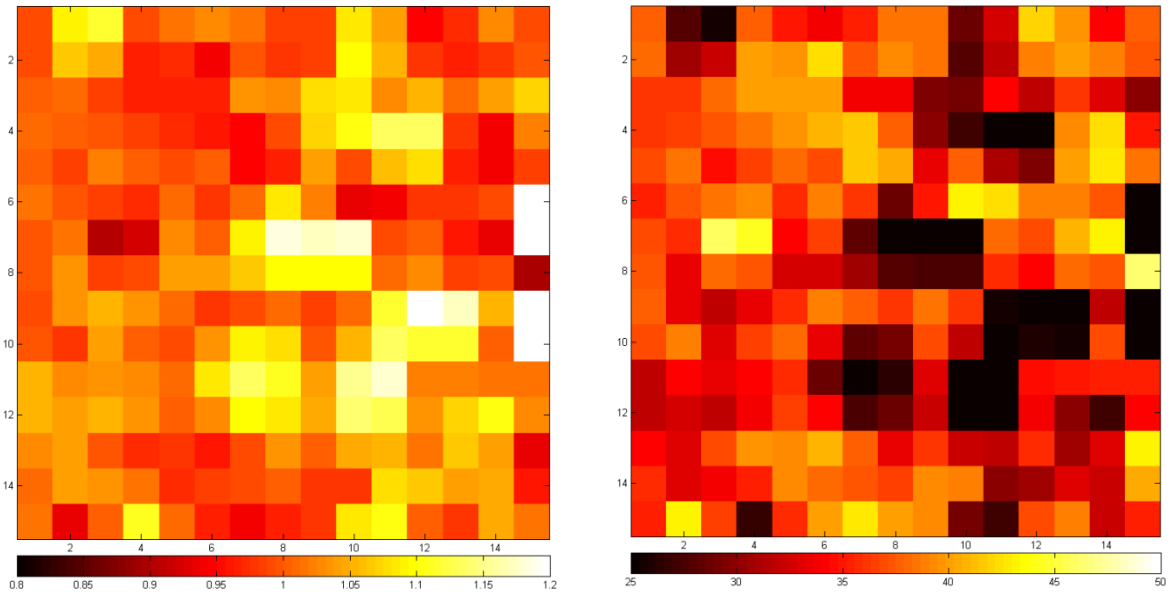

Figure 7.9 Intensity ratio map (left) and temperature map (right)

The temperature map in Figure 7.9, with the colorbar showing a temperature range from 25-50ºC, generally indicates a region of warmer fluid in the buoyant plume at the left, and colder fluid outside of the plume. Inaccuracies in the temperature map are largely due to imprecision in camera alignment. Additionally, particle streaking and small discrepancies in the simultaneity of images contribute to errors. Despite these difficulties, the simultaneous thermometry and velocimetry capability of the E-H #3 TSBs was demonstrated. With improvements to the experimental setup and the use of faster cameras, the thermometric accuracy will increase significantly.

Chapter 8. CONCLUSIONS

Collaborative efforts between the University of Washington and Washington University in St. Louis have led to the development of temperature-sensitive beads with promising characteristics for complex flow visualization via simultaneous full-field thermometry and velocimetry. While the luminescent and physical requirements for satisfactorily-functioning TSBs are ultimately dependent on the specific flow of interest, the TSB development in this research effort has resulted in TSBs that have suitable features for application to a variety of complex water flows.

For the natural convection flow discussed, the E-H #3 TSBs have been shown to meet particle size, particle response time, particle density, and temperature sensitivity requirements. A thermal response time for the TSBs has yet to be measured. In depth research into the measurement of thermal response time revealed that the shock tube may not be an appropriate apparatus for imparting an instantaneous temperature change. Impartation of an instantaneous temperature change proves to be rather challenging in practice, and a thorough literature survey showed successful execution in only one study [16]. Laser pulse heating using an infrared laser is a proposed technique that warrants further consideration and investigation.

Flow visualization of natural convection in water was performed using a number of luminescent TSBs, but the best results were achieved for the E-H #3 TSBs. Images of the E-H #3 TSBs were first captured and processed to provide a qualitative temperature field as well as quantitative PIV results. Subsequently, simultaneous E and H dye images were captured and a temperature calibration was completed to implement in correction of non-uniformities. Application of the calibration led to quantitative temperature field results. Although temperature accuracy is currently relatively low, improvements to the experimental apparatus and imaging equipment will have significant impact.

Although it was presupposed that particle uniformity is not essential, flow visualization tests generally showed otherwise. Uniformity in reference dye doping and particle size/shape is important so that consistent luminescence occurs, allowing for adequate detection without data loss due to bright outlier particles.

With the cameras and equipment used in this experimental effort, particle streaking occurred for natural convection even at maximum camera speed. In order to achieve the temporal

resolution desired to fully resolve turbulent flows, high-speed cameras with faster imaging capabilities than those used in this research effort are required and should be attained.

Although the TSBs and corresponding imaging processes are not, at this moment, fully-developed for turbulent flow visualization, the necessary TSB characteristics are approaching fulfillment and should be achieved in the near future.

BIBLIOGRAPHY

[1] P. Childs, Practical Temperature Measurement, Oxford: Butterworth-Heinemann, 2001.

[2] R. McIntosh, "A Microsecond Response Thermocouple For Use in the Ram Accelerator," University of Washington, 1991.

[3] B. Lawton and G. Klingenberg, Transient Temperature in Engineering and Science, New York: Oxford UP, 1996.

[4] J. Gallery, M. Gouterman, J. Callis, G. Khalil, B. McLachlan and J. Bell, "Luminescent thermometry for aerodynamic measurements," *Rev. Sci. Instrum.,* vol. 65, no. 3, pp. 712-720, 1994.

[5] T. Liu and J. Sullivan, Pressure and Temperature Sensitive Paints, Berlin: Springer-Verlag, 2005.

[6] M. Raffel, C. Willert and J. Kompenhans, Particle Image Velocimetry, Berlin: Springer-Verlag, 1998.

[7] D. Dabiri, "Digital particle image thermometry/velocimetry: a review," *Exp Fluids,* pp. 191-241, 2008.

[8] H. Park, "A study of heat transport processes in the wake of a stationary oscillating circular cylinder using digital particle image velocimetry/thermometry," California Institute of Technology, Pasadena, 1998.

[9] H. Park and M. Gharib, "Experimental study of heat convection from stationary and oscillating circular cylinder in cross flow," *J Heat Transf,* pp. 51-62, 2001.

[10] H. Park, D. Dabiri and M. Gharib, "Digital particle image velocimetry/thermometry and application to the wake of a heated circular cylinder," *Exp Fluids,* vol. 30, pp. 327-338, 2001.

[11] S. Someya, Y. Li, K. Ishii and K. Okamoto, "Combined two-dimensional velocity and temperature measurements of natural convection using a high-speed camera and temperature-sensitive particles," *Exp Fluids,* pp. 65-73, 2010.

[12] R. Adrian and J. Westerweel, Particle Image Velocimetry, New York: Cambridge UP, 2011.

[13] H. Liepmann and A. Roshko, Elements of Gasdynamics, New York: John Wiley & Sons, Inc., 1957.

[14] F. Kimura, M. Rodriguez, J. McCann, B. Carlson, D. Dabiri, G. Khalil, J. Callis, Y. Xia and M. Gouterman, "Development and characterization of fast responding pressure sensitive microspheres," *Rev Sci Instrum,* vol. 79, 2008.

[15] F. Kimura, "Novel Measurement Techniques for the Study of Unsteady Flow Phenomena: Shear Sensitive Paint and Pressure Sensitive Microspheres," University of Washington, 2009.

[16] T. Liu, B. Campbell, S. Bruns and J. Sullivan, "Temperature- and pressure-sensitive luminescent paints in aerodynamics," *Applied Mechanics Reviews,* vol. 50, no. 4, pp. 227-246, 1997.

[17] S. Yang, "Improvement of the basic correlating equations and transition criteria of natural

convection heat transfer," *Heat Transfer - Asian Res.,* vol. 30, pp. 293-300, 2001.
[18] F. White, Viscous Fluid Flow, New York: McGraw-Hill, 1991.